

Supporting Information for:

Pollen-like ZIF-8 colloidosomes via emulsion templating and etching

Lucia-Lupica Spagnolo, Daniel J. Ward, John-Joseph Marie, Smaragda Lympieropoulou and
Darren Bradshaw*

School of Chemistry, University of Southampton, Southampton SO17 1BJ, U.K.

e-mail: d.bradshaw@soton.ac.uk

Synthetic methods

General synthesis of ZIF-8 colloidosomes

Typically, 90 mg of SPAN-80 and 25 μL of dodecane were dispersed in 5 mL of DI water using ultrasound for 10 min. A stable emulsion was generated by agitation using a shear force instrument at 11500 rpm for 2 min. Then a solution of $\text{Zn}(\text{NO}_3)_2 \cdot 6\text{H}_2\text{O}$ (0.029g in 0.5 mL H_2O) was added to the emulsion and stored at 4 °C for 3 hrs, after which time a 2-methyl imidazole (2-Melm) (0.56g in 2 mL H_2O) solution was further added and the synthesis mixture kept at 4° C overnight. The white precipitate was recovered by centrifugation at 5000 rpm, washed twice with ethanol and dried at r.t. overnight prior to analysis. Yield = 15 mg

The same procedure was followed in all cases, with adjustment of the amount of SPAN-80 (18 – 162 mg), shear speed (9,500 and 14,500 rpm) and shear time (1 and 10 mins) depending on which variable was under investigation. The corresponding ZIF-67 capsules were synthesised by using $\text{Co}(\text{NO}_3)_2 \cdot 6\text{H}_2\text{O}$ in place of the zinc salt.

When no SPAN-80 was used the best results were obtained when the ZIF-8 precursors were added immediately and sequentially ($\text{Zn}(\text{NO}_3)_2$ then 2-Melm) following emulsification without the 3 hr wait. This strategy can also be employed when SPAN-80 is present.

Etching of ZIF-8 colloidosomes

0.46 g of imidazole was dissolved in 7 mL of DI water (0.97 M) and then added to 15 mg of the ZIF-8 colloidosomes and left to stand for a defined period. The solid material was recovered by centrifugation at 5000 rpm, washed twice with ethanol and dried at r.t. overnight prior to analysis.

For the other etchants employed (1-methyl-imidazole, pyrazole and pyrimidine) similar molar solutions were prepared.

Characterisation

Powder X-ray diffraction (PXRD) patterns were collected on a Bruker D2-phaser diffractometer in the angular range $2\theta = 5- 50^\circ$ employing a Ni $\text{K}\beta$ filter (detector side) producing Cu ($\text{K}\alpha_1/\text{K}\alpha_2$) radiation.

Scanning Electron Microscopy (SEM) images were made on a JEOL JSM 6500 thermal field emission scanning electron microscope at an accelerating voltage of 10 kV. Samples for SEM measurements were prepared by firstly placing a drop of sample suspension in absolute ethanol on a silica wafer attached to an aluminium substrate with a carbon paste, and then sputter-coated with a thin layer of conductive gold to improve electrical conductivity.

$^1\text{H-NMR}$ spectra were acquired using a Bruker DPX400 FT-NMR spectrometer following digestion of the samples using HCl.

Fourier Transform Infrared (FTIR) spectra were collected on a Magna IR-560 Nicolet FTIR spectrometer equipped with a Mercure Cadmium Tellure detector. All experiments were run

on a horizontal attenuated total reflectance (ATR) crystal (ZnSe) where powders were pressed. Content of metals was analysed using a Varian Vista MPX.

N₂ adsorption/desorption isotherms were measured at 77 K using a Micromeritics 3-Flex Surface Characterization Analyzer after the sample was first degassed at 100°C overnight. Surface areas were determined by the BET method in an appropriate pressure range, and total pore volume was determined using the adsorption branch of N₂ isotherm curve at the $p/p_0 = 0.99$ single point. Pore size distribution was determined using the adsorption branch of N₂ isotherms. Mesopore size distribution was calculated using the Barrett-Joyner-Halenda (BJH) method.

Thermogravimetric analysis (TGA) was performed using a TG 209 F1 Libra (Netzsch) and typically the sample was heated from room temperature to 900°C at a rate of 10°C min⁻¹ under an air atmosphere.

Additional figures

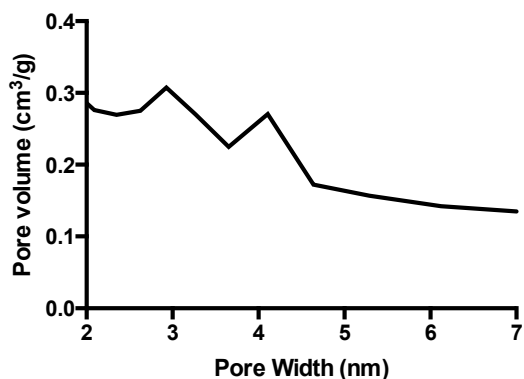


Figure S1. BJH (desorption) pore size distribution for emulsion-templated ZIF-8 colloidosomes prepared in the presence of 90 mg SPAN-80.

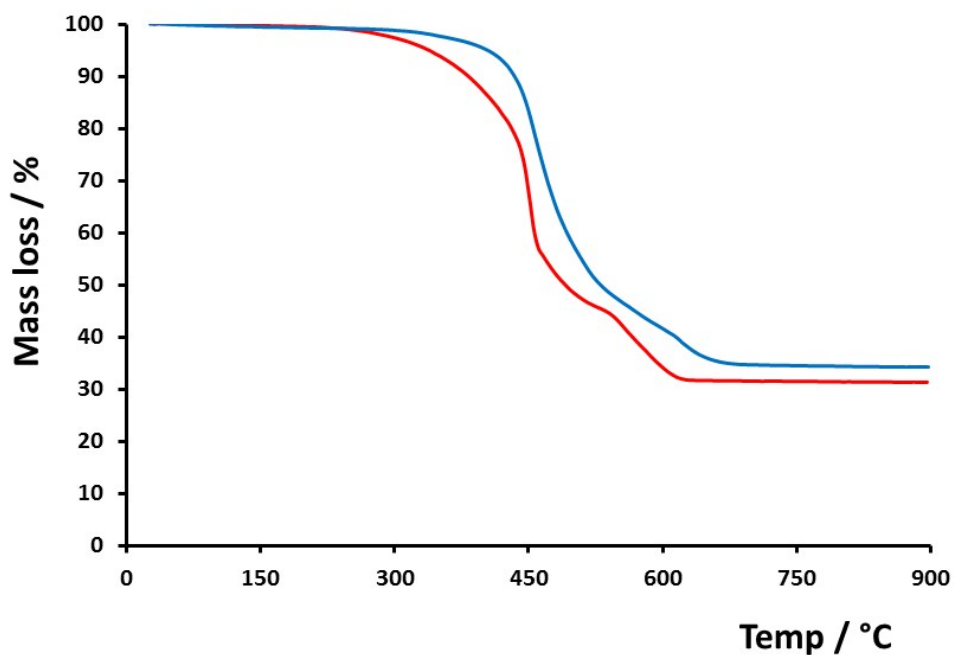


Figure S2. TGA mass loss profile of emulsion-templated ZIF-8 colloidosomes prepared in the presence of 90 mg SPAN-80 (red), compared to a bulk sample of ZIF-8 (blue). The organic mass loss for the colloidosomes is 68% compared to the expected 64% for the bulk sample, indicating the presence of a small amount of residual surfactant.

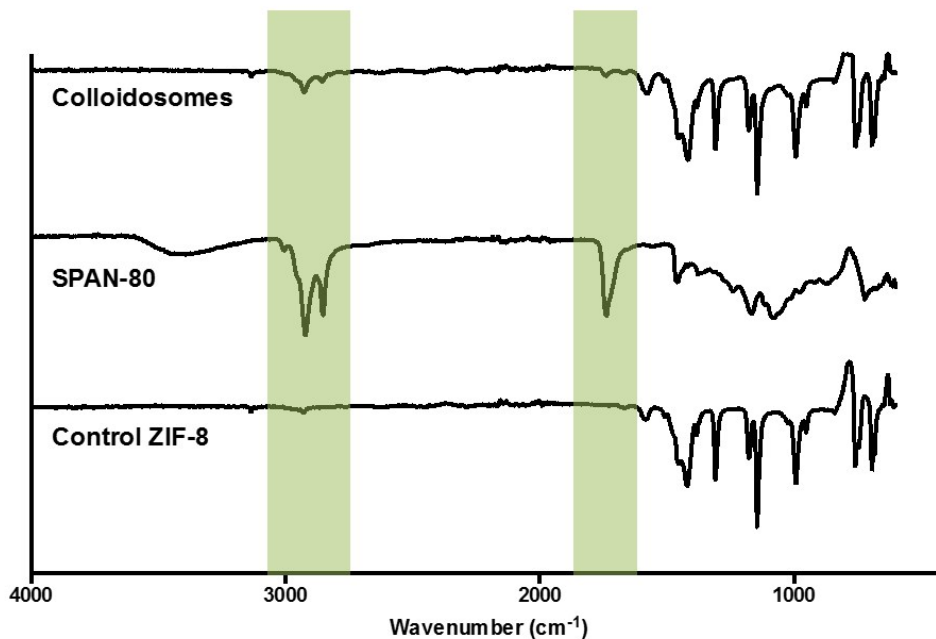


Figure S3. FTIR spectra of emulsion-templated ZIF-8 colloidosomes prepared in the presence of 90 mg SPAN-80, compared to a bulk (control) sample of ZIF-8 and SPAN-80 alone.

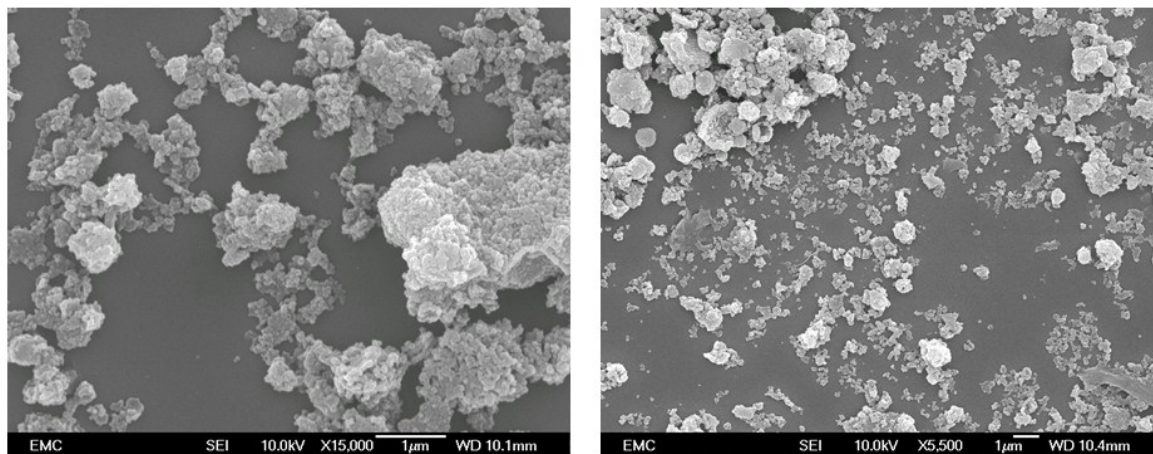


Figure S4. Representative SEM images of ZIF-8 formed in the presence of SPAN-80 and dodecane without the application of shear force. In this case a magnetic stirrer-bar was employed and it is clear that colloidosomes cannot be templated under these conditions.

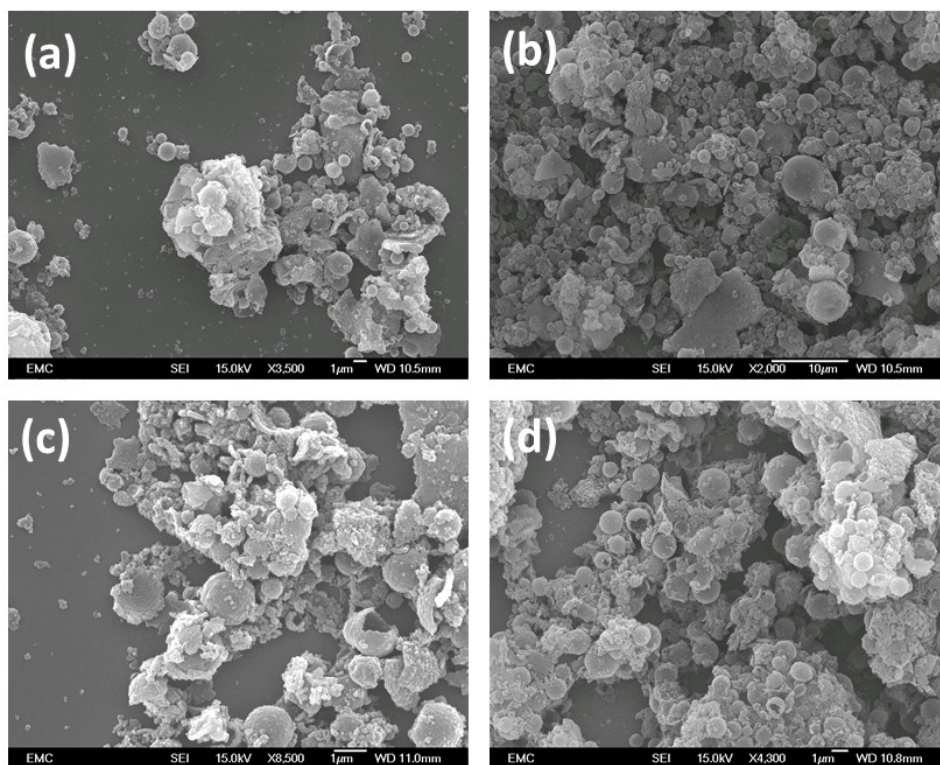
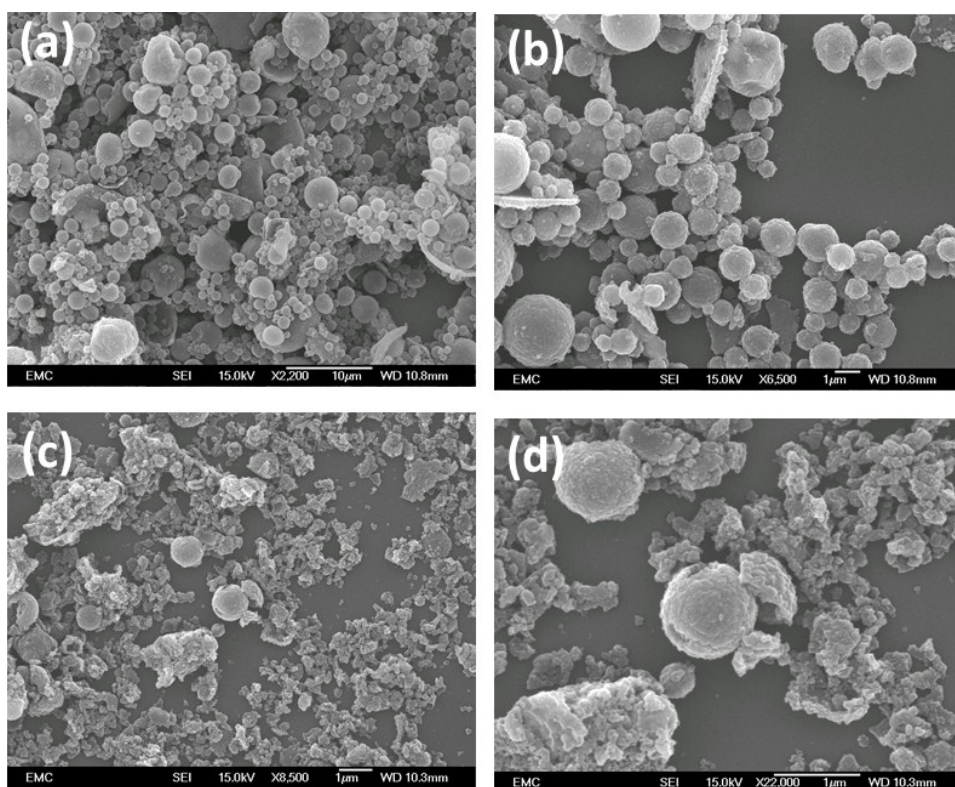


Figure S5. SEM images of ZIF-8 colloidosomes prepared at different shear speeds (a,b) 2 mins



at 9,000 rpm and (c,d) 2 mins at 14,500 rpm.

Figure S6. SEM images of ZIF-8 colloidosomes prepared at different shear times at a constant speed of 11,500 rpm (a,b) 1 min and (c,d) 10 mins.

SAMPLE	a	b	c	d	e	f
DODECANE (μl)	25	25	25	25	25	25
SPAN-80 (mg)	0	18	54	90	126	162

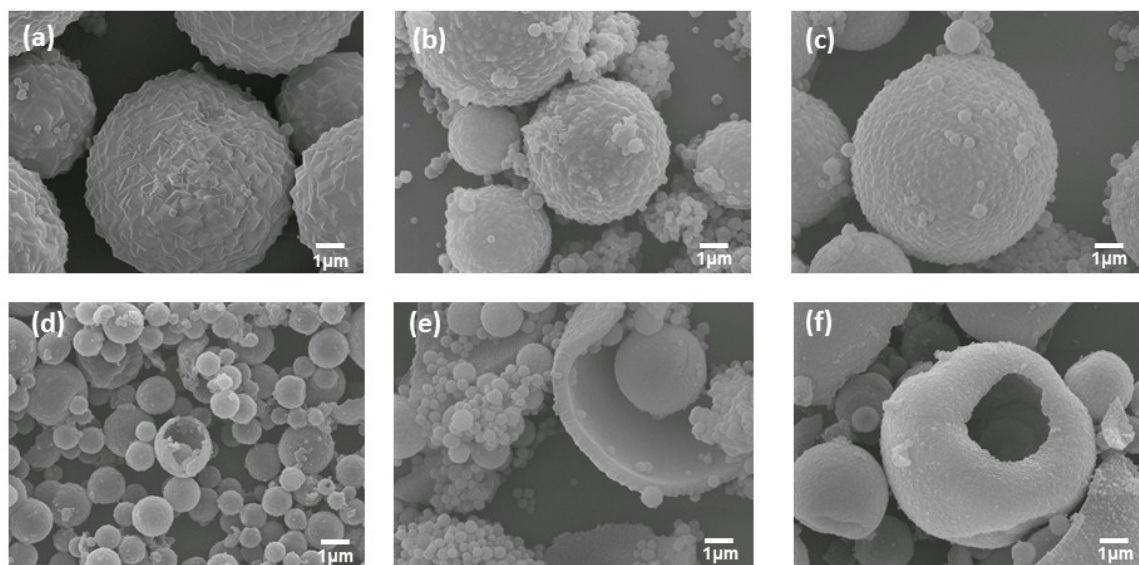
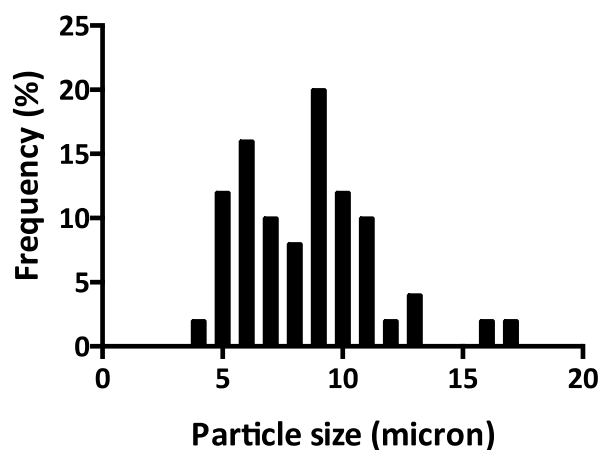


Figure S7. SEM images revealing the effect of changing the amount of SPAN-80 surfactant on the capsules at a fixed volume of the dodecane internal phase. The standard condition is shown in (d), and at all levels of SPAN-80 investigated well-defined ZIF-8 colloidosomes were



formed.

Figure S8. Size distribution for ZIF-8 capsules prepared in the absence of SPAN-80. The data indicate that the size of the capsules are approx. 1 order of magnitude greater than those prepared with the surfactant (as shown in the inset of figure 1a in the manuscript).

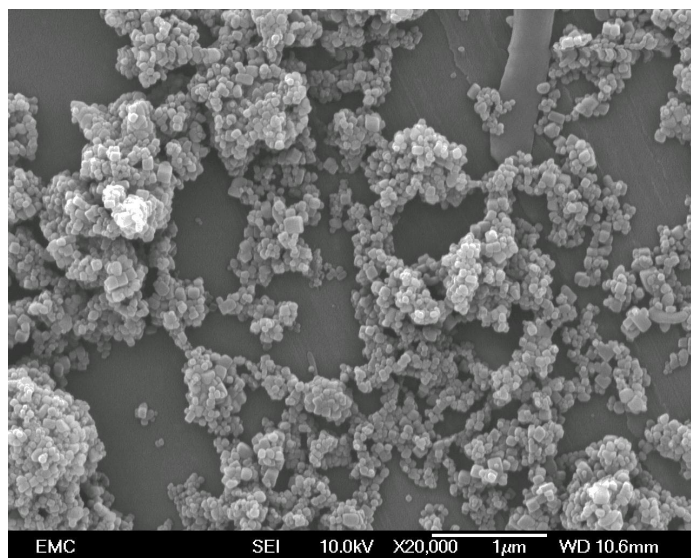


Figure S9. SEM image of ZIF-8 nanocrystals prepared in the presence of SPAN-80 as an additive. See also figure S4.

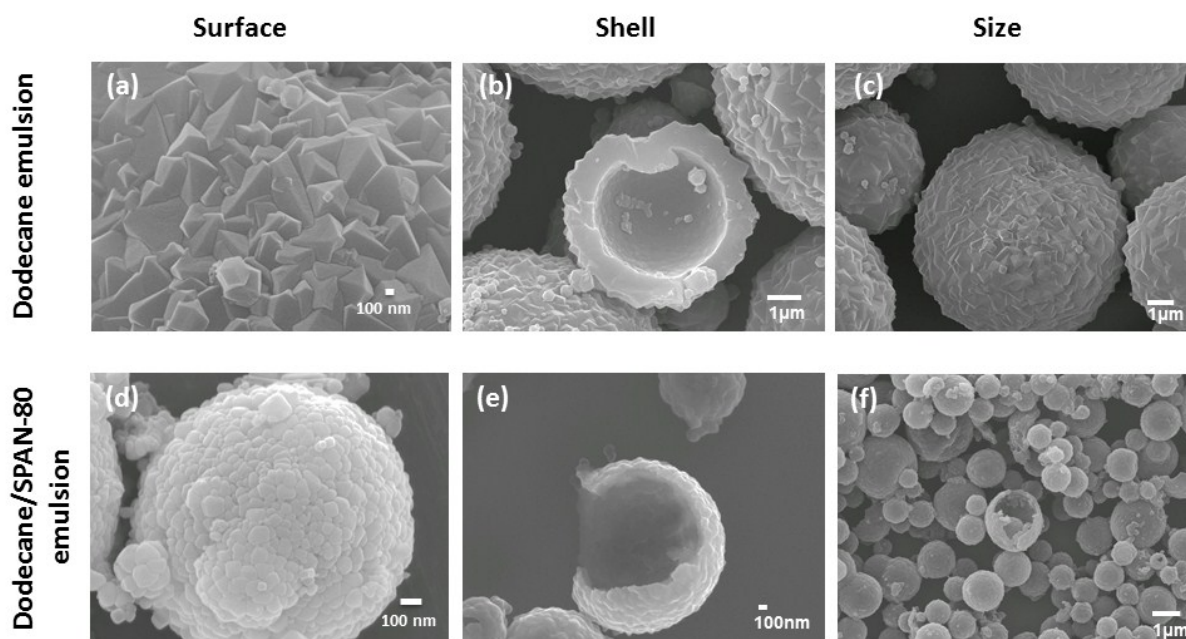


Figure S10. Comparison of capsule dimensions, shell thickness and surface roughness in the absence and presence of SPAN-80 as an emulsifier. SEM images for the dodecane/SPAN-80 system correspond to the standard condition (90 mg SPAN-80).

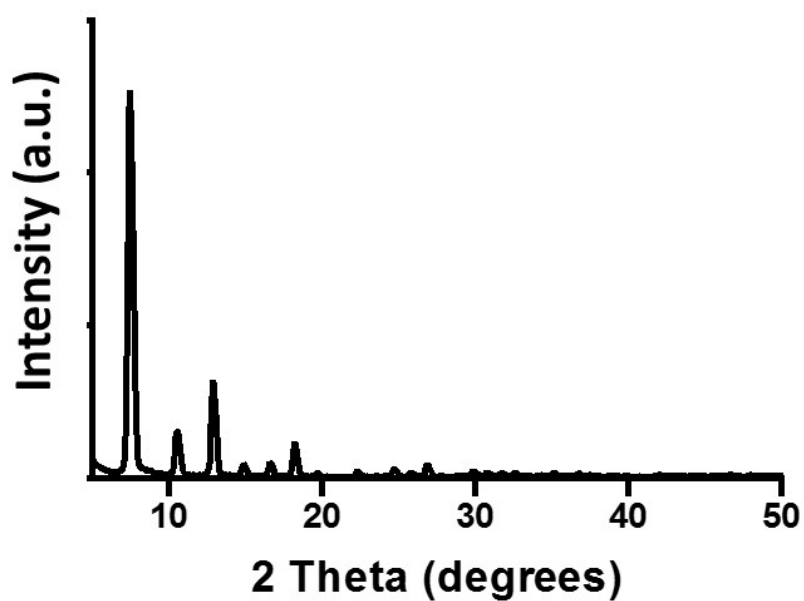


Figure S11. PXRD of emulsion-templated ZIF-8 colloidosomes prepared using dodecane only.

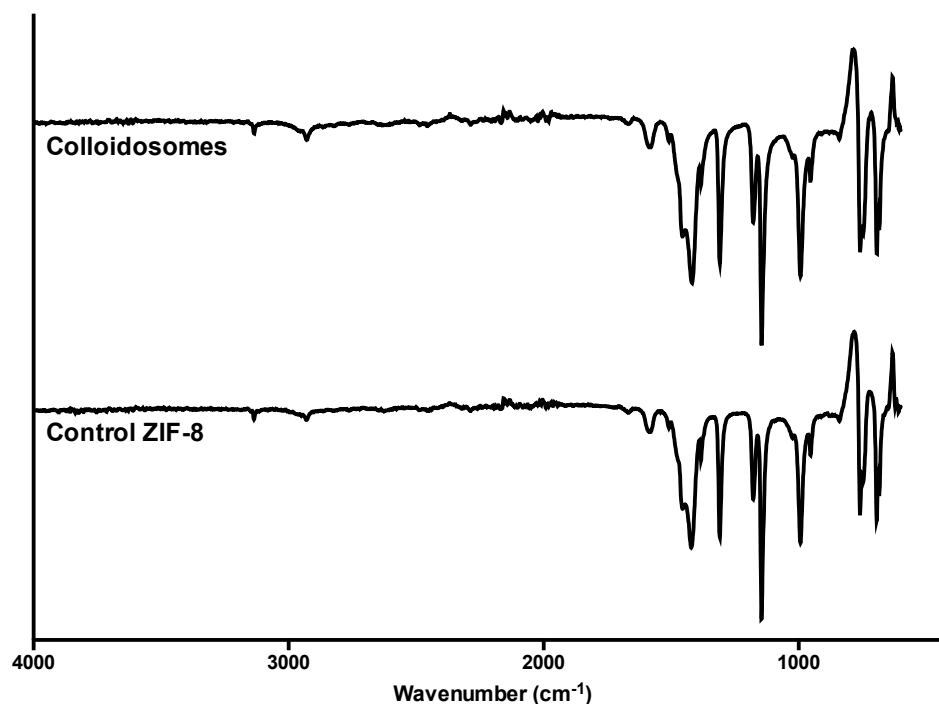


Figure S12. FTIR spectra of emulsion-templated ZIF-8 colloidosomes prepared using dodecane only, compared to a bulk (control) sample of ZIF-8.

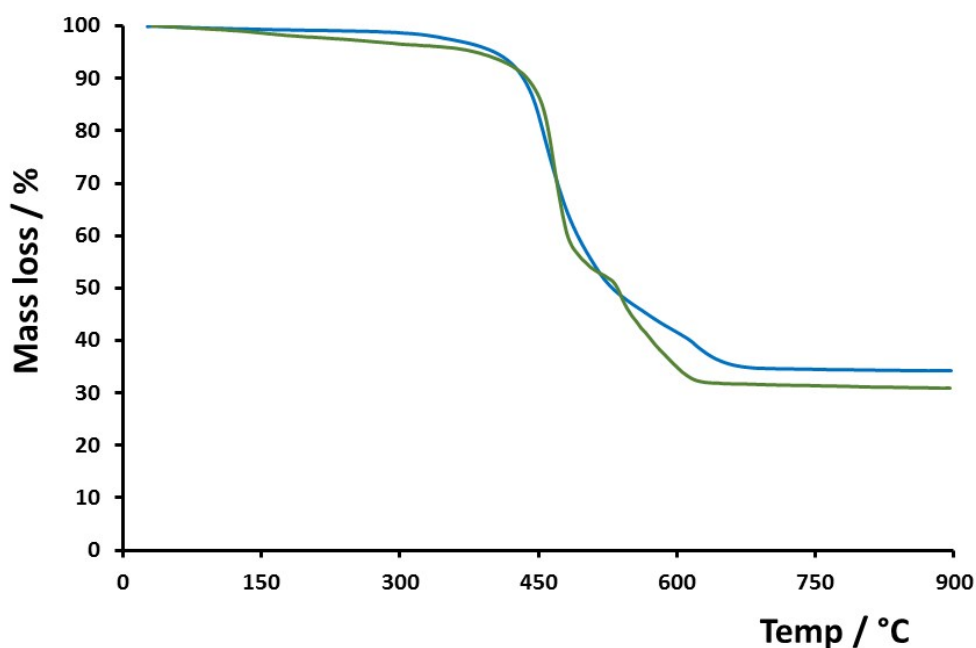


Figure S13. TGA mass loss profile of surfactant-free emulsion-templated ZIF-8 colloidosomes (green), compared to a bulk sample of ZIF-8 (blue). The organic mass loss for the colloidosomes following solvent removal is 64.5% in excellent agreement with the expected 64% and that observed for the bulk sample. The relatively small but gradual loss between 150 – 350 °C for the colloidosomes is attributed to a small amount of included dodecane.

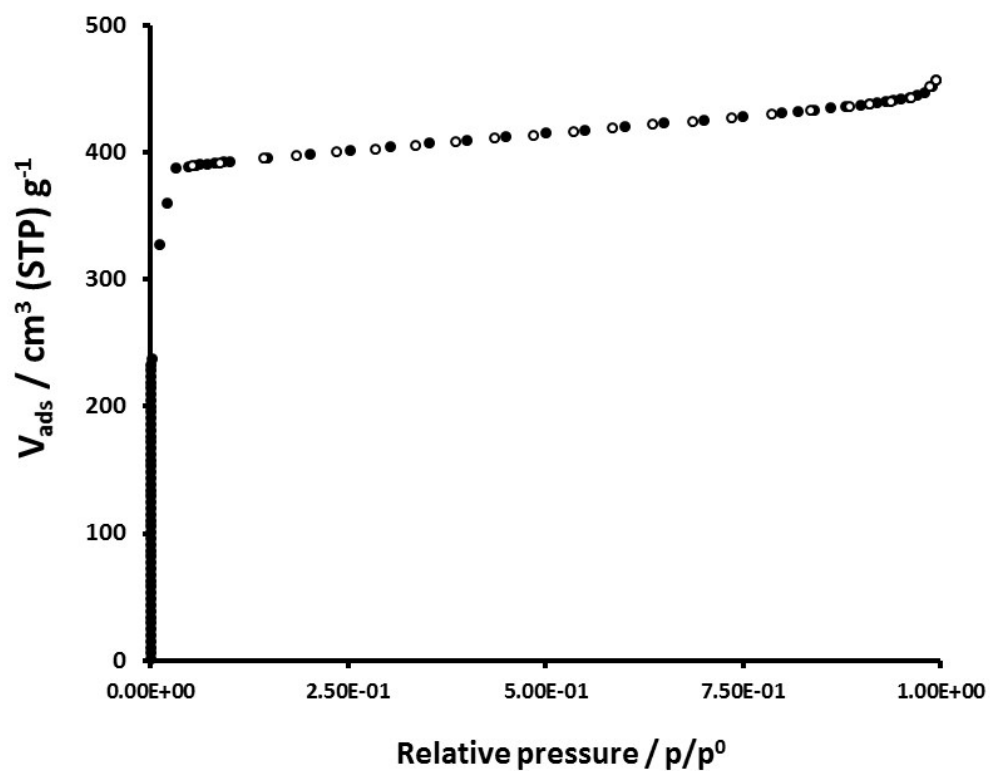


Figure S14. Nitrogen adsorption isotherm (77 K) for surfactant-free emulsion-templated ZIF-8 colloidosomes.

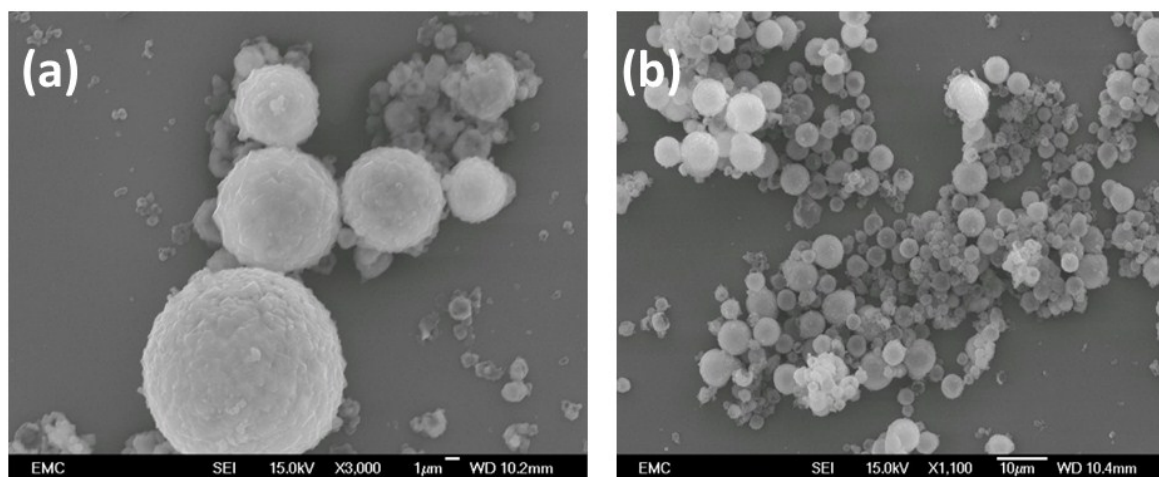


Figure S15. SEM images of ZIF-67 colloidosomes formed (a) in the presence of SPAN-80 and (b) under surfactant-free conditions.

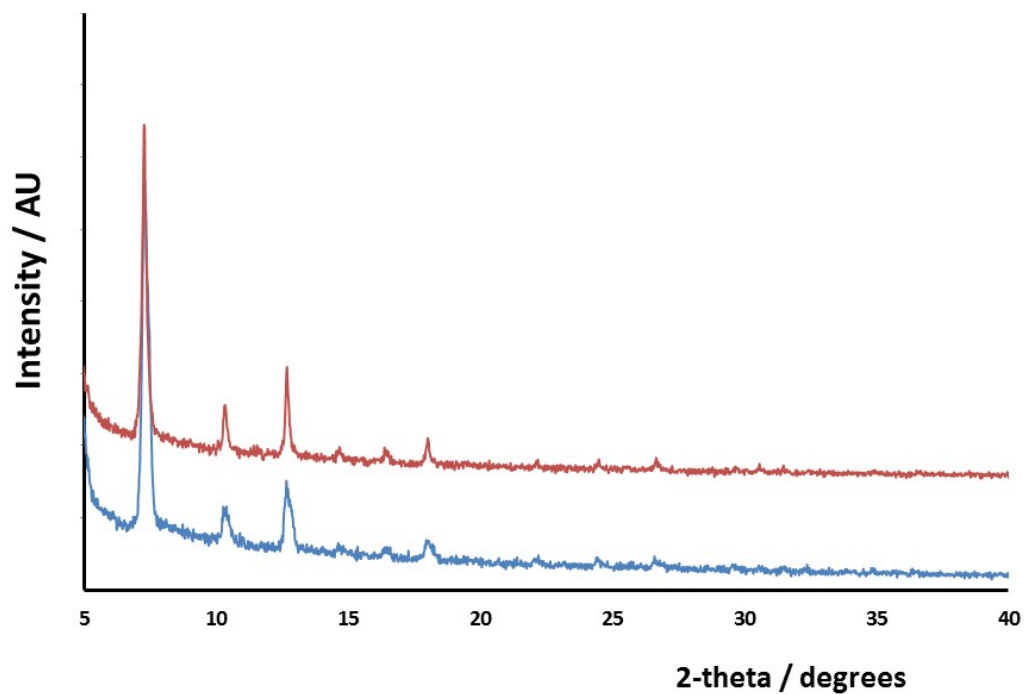


Figure S16. PXRD data for emulsion-templated ZIF-67 colloidosomes prepared without (blue) and with (red) SPAN-80.

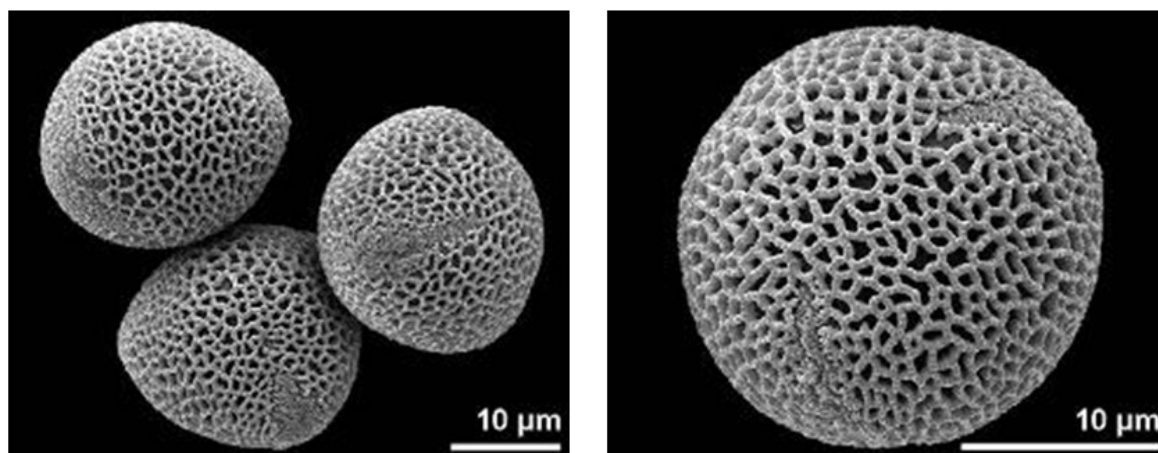


Figure S17. SEM images of *Oleaceae* pollen grains. Images reproduced with permission from and acknowledgement to Heidemarie Halbritter and PalDat (2000 onwards, www.paldat.org).

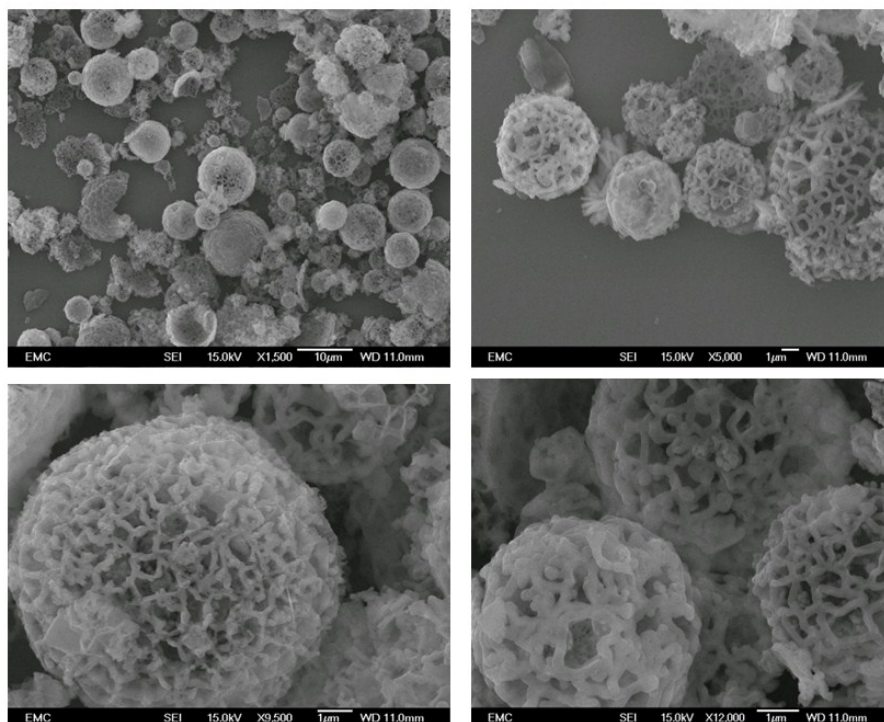


Figure S18. SEM images of ZIF-67 colloidosomes etched using 1M aqueous imidazole for 15 minutes.

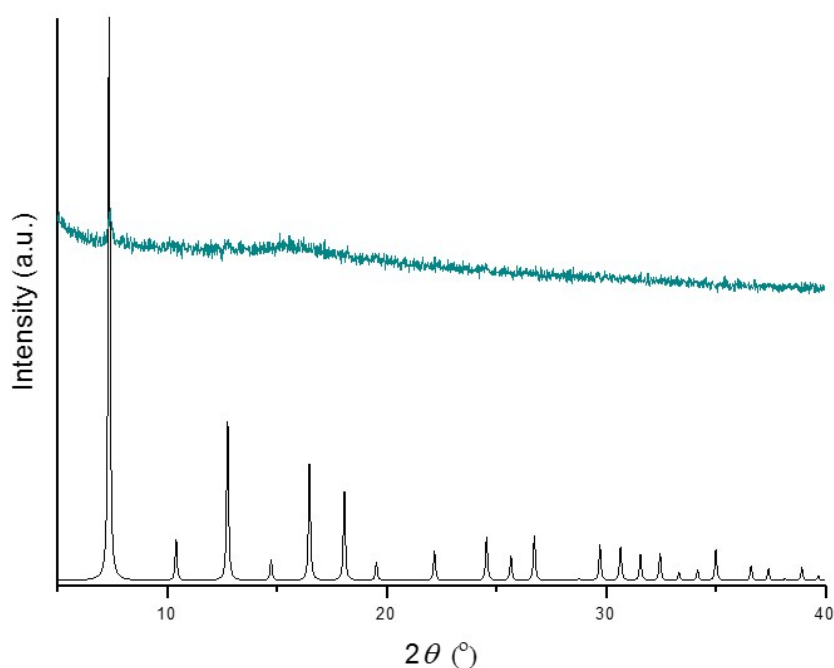


Figure S19. Typical PXRD pattern of ZIF-67 colloidosomes (top) following etching by 1M aqueous imidazole for 15 minutes, showing this is largely amorphous *cf.* the sodalite reference pattern (bottom).

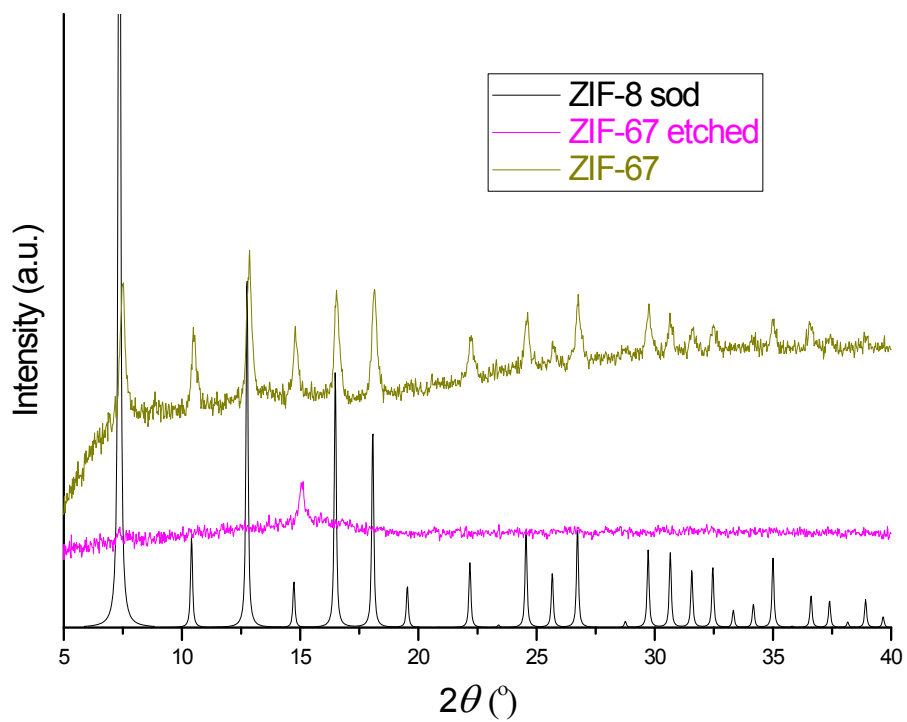


Figure S20. PXRD patterns of bulk ZIF-67 before and after etching for 30 mins in a 1M solution of aqueous imidazole.

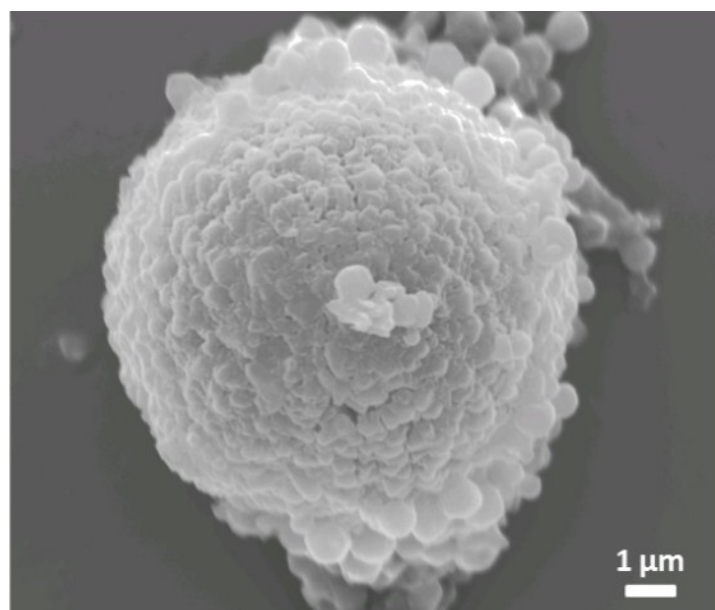
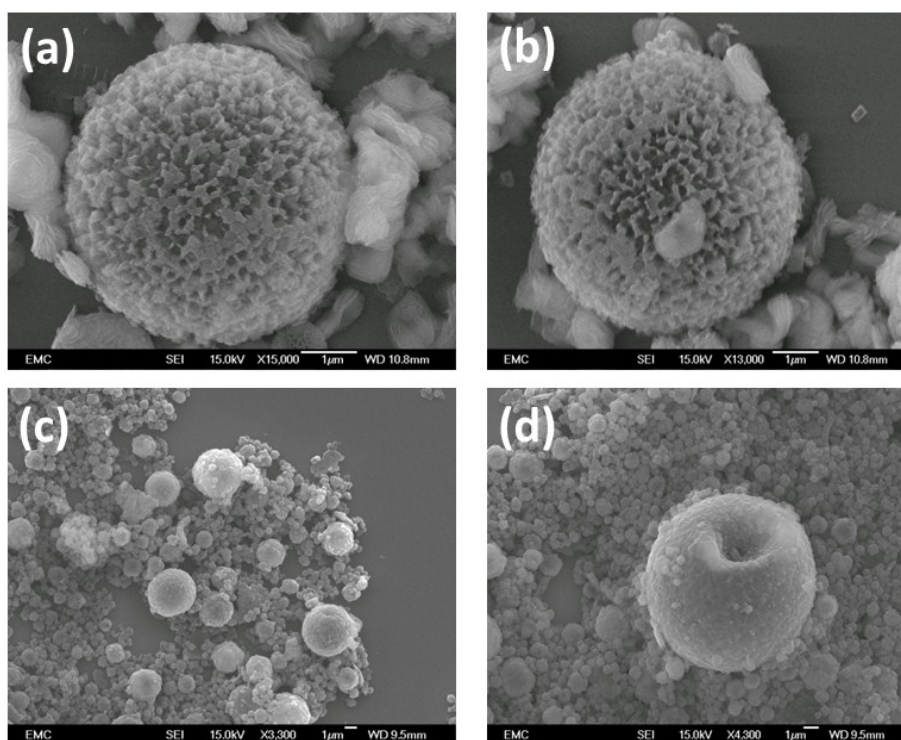


Figure S21. Representative SEM image of ZIF-8 colloidosomes following etching with 1-Melm



in water for 2 hrs, demonstrating the importance of N-H acidity.

Figure S22. SEM images of ZIF-8 colloidosomes etched with (a, b) 1M aqueous pyrazole and (c,d) 1M aqueous pyrimidine; scale bars 1μm in all images. There are a number of free ZIF-8 crystals present in the samples etched with pyrimidine due to the original synthesis conditions, whereas a number of crystals with a morphology not consistent with a $\text{Zn}(\text{Melm})_2$ phase are observed when pyrazole was employed as etchant.

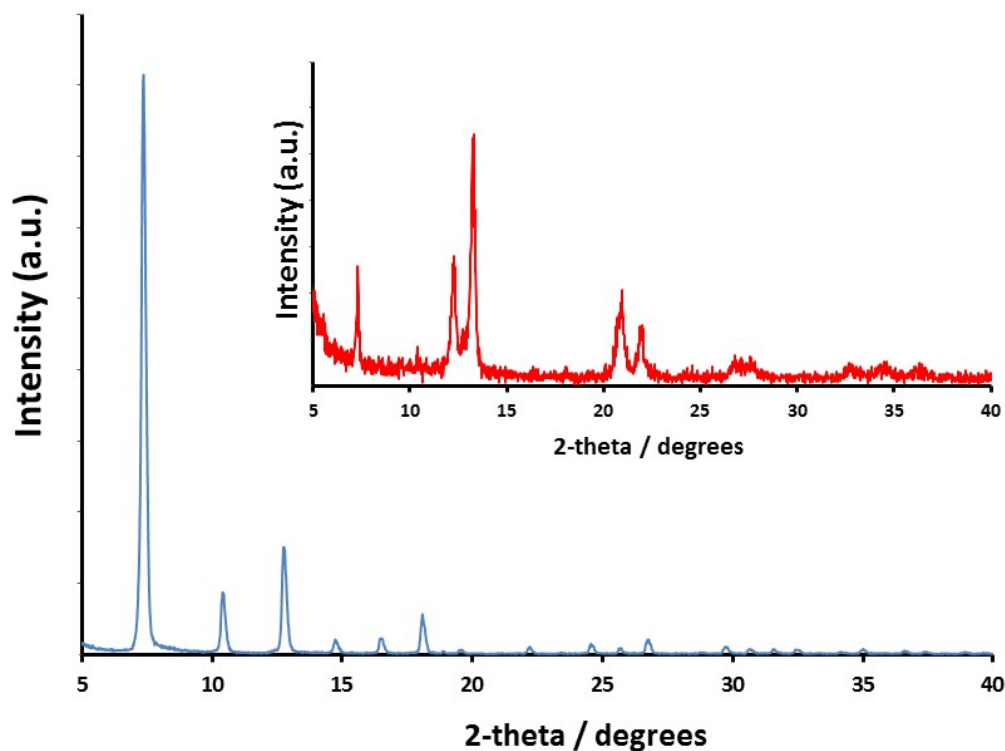


Figure S23. PXRD data of ZIF-8 colloidosomes following etching with aqueous pyrimidine (blue, main trace) and pyrazole (red, inset). The diffraction pattern observed following pyrazole etching most likely corresponds to an as yet unidentified Zn-pyrazole phase consistent with the unexpected (*viz.* not sod or zni) morphology of the free crystals observed in SEM images (figure S20).